

AERO. & ASTRO. LIBRARY



NATIONAL ADVISORY COMMITTEE
FOR AERONAUTICS

Copy #3

REPORT No. 914

EFFECT OF CENTRIFUGAL FORCE ON THE ELASTIC
CURVE OF A VIBRATING CANTILEVER BEAM

By SCOTT H. SIMPKINSON, LAUREL J. EATHERTON

and MORTON B. MILLENSON



1948

For sale by the Superintendent of Documents, U. S. Government Printing Office, Washington 25, D. C. Yearly subscription, \$3; foreign, \$4.50;
single copy price varies according to size. - - - - - Price 15 cents

623.742
U 58-

AERONAUTIC SYMBOLS

1. FUNDAMENTAL AND DERIVED UNITS

| Symbol | Metric | | | English | |
|------------|---|--------------|-----------------------------------|--------------|--------------|
| | Unit | Abbreviation | Unit | Abbreviation | Abbreviation |
| Length l | meter | m | foot (or mile) | ft (or mi) | |
| Time t | second | s | second (or hour) | sec (or hr) | |
| Force F | weight of 1 kilogram | kg | weight of 1 pound | lb | |
| Power P | horsepower (metric) | | horsepower | hp | |
| Speed V | {kilometers per hour {meters per second} | kph mps | miles per hour feet per second | mph fps | |

2. GENERAL SYMBOLS

| | | |
|-------|--|--|
| W | Weight = mg | Kinematic viscosity |
| g | Standard acceleration of gravity = 9.80665 m/s^2 or 32.1740 ft/sec^2 | Density (mass per unit volume) |
| m | Mass = $\frac{W}{g}$ | Standard density of dry air, $0.12497 \text{ kg-m}^{-4} \text{-s}^2$ at 15° C and 760 mm; or $0.002378 \text{ lb-ft}^{-4} \text{ sec}^2$ |
| I | Moment of inertia = mk^2 . (Indicate axis of radius of gyration k by proper subscript.) | Specific weight of "standard" air, 1.2255 kg/m^3 or 0.07651 lb/cu ft |
| μ | Coefficient of viscosity | |

3. AERODYNAMIC SYMBOLS

| | | | |
|-------|--|-----------------|--|
| S | Area | i_w | Angle of setting of wings (relative to thrust line) |
| S_w | Area of wing | i_t | Angle of stabilizer setting (relative to thrust line) |
| G | Gap | Q | Resultant moment |
| b | Span | Ω | Resultant angular velocity |
| c | Chord | R | Reynolds number, $\rho \frac{Vl}{\mu}$ where l is a linear dimen- sion (e.g., for an airfoil of 1.0 ft chord, 100 mph, standard pressure at 15° C , the corresponding Reynolds number is 935,400; or for an airfoil of 1.0 m chord, 100 mps, the corresponding Reynolds number is 6,865,000) |
| A | Aspect ratio, $\frac{b^2}{S}$ | α | Angle of attack |
| V | True air speed | ϵ | Angle of downwash |
| q | Dynamic pressure, $\frac{1}{2} \rho V^2$ | α_∞ | Angle of attack, infinite aspect ratio |
| L | Lift, absolute coefficient $C_L = \frac{L}{qS}$ | α_i | Angle of attack, induced |
| D | Drag, absolute coefficient $C_D = \frac{D}{qS}$ | α_a | Angle of attack, absolute (measured from zero- lift position) |
| D_0 | Profile drag, absolute coefficient $C_{D_0} = \frac{D_0}{qS}$ | γ | Flight-path angle |
| D_i | Induced drag, absolute coefficient $C_{D_i} = \frac{D_i}{qS}$ | | |
| D_p | Parasite drag, absolute coefficient $C_{D_p} = \frac{D_p}{qS}$ | | |
| C | Cross-wind force, absolute coefficient $C_c = \frac{C}{qS}$ | | |

REPORT No. 914

EFFECT OF CENTRIFUGAL FORCE ON THE ELASTIC CURVE OF A VIBRATING CANTILEVER BEAM

By SCOTT H. SIMPKINSON, LAUREL J. EATHERTON
and MORTON B. MILLENSON

Aircraft Engine Research Laboratory
Cleveland, Ohio

I

National Advisory Committee for Aeronautics

Headquarters, 1724 F Street NW, Washington 25, D. C.

Created by act of Congress approved March 3, 1915, for the supervision and direction of the scientific study of the problems of flight (U. S. Code, title 50, sec. 151). Its membership was increased to 17 by act approved May 25, 1948. (Public Law 549, 80th Congress). The members are appointed by the President, and serve as such without compensation.

JEROME C. HUNSAKER, Sc. D., Cambridge, Mass., *Chairman*

ALEXANDER WETMORE, Sc. D., Secretary, Smithsonian Institution, *Vice Chairman*

HON. JOHN R. ALISON, Assistant Secretary of Commerce.
DETLEV W. BRONK, Ph. D., President, Johns Hopkins University.
KARL T. COMPTON, Ph. D. Chairman, Research and Development

Board, National Military Establishment.

EDWARD U. CONDON, Ph. D., Director, National Bureau of Standards.

JAMES H. DOOLITTLE, Sc. D., Vice President, Shell Union Oil Corp.

R. M. HAZEN, B. S., Director of Engineering, Allison Division, General Motors Corp.

WILLIAM LITTLEWOOD, M. E., Vice President, Engineering, American Airlines, Inc.

THEODORE C. LONNQUEST, Rear Admiral, United States Navy, Assistant Chief for Research and Development, Bureau of Aeronautics.

EDWARD M. POWERS, Major General, United States Air Force, Assistant Chief of Air Staff-4.

JOHN D. PRICE, Vice Admiral, United States Navy, Deputy Chief of Naval Operations (Air).

ARTHUR E. RAYMOND, M. S., Vice President, Engineering, Douglas Aircraft Co., Inc.

FRANCIS W. REICHELDERFER, Sc. D., Chief, United States Weather Bureau.

HON. DELOS W. RENTZEL, Administrator of Civil Aeronautics, Department of Commerce.

HOYT S. VANDENBERG, General, Chief of Staff, United States Air Force.

THEODORE P. WRIGHT, Sc. D., Vice President for Research, Cornell University.

HUGH L. DRYDEN, Ph. D., *Director of Aeronautical Research*

JOHN F. VICTORY, LL.M., *Executive Secretary*

JOHN W. CROWLEY, JR., B. S., *Associate Director of Aeronautical Research*

E. H. CHAMBERLIN, *Executive Officer*

HENRY J. E. REID, Eng. D., Director, Langley Aeronautical Laboratory, Langley Field, Va.

SMITH J. DEFRENCE, B. S., Director, Ames Aeronautical Laboratory, Moffett Field, Calif.

EDWARD R. SHARP, Sc. D., Director, Lewis Flight Propulsion Laboratory, Cleveland Airport, Cleveland, Ohio

TECHNICAL COMMITTEES

AERODYNAMICS
POWER PLANTS FOR AIRCRAFT
AIRCRAFT CONSTRUCTION

OPERATING PROBLEMS
INDUSTRY CONSULTING

*Coordination of Research Needs of Military and Civil Aviation
Preparation of Research Programs
Allocation of Problems
Prevention of Duplication
Consideration of Inventions*

LANGLEY AERONAUTICAL LABORATORY,
Langley Field, Va.

LEWIS FLIGHT PROPULSION LABORATORY,
Cleveland Airport, Cleveland, Ohio

AMES AERONAUTICAL LABORATORY,
Moffett Field, Calif.

Conduct, under unified control, for all agencies, of scientific research on the fundamental problems of flight

OFFICE OF AERONAUTICAL INTELLIGENCE,
Washington, D. C.

Collection, classification, compilation, and dissemination of scientific and technical information on aeronautics

REPORT No. 914

EFFECT OF CENTRIFUGAL FORCE ON THE ELASTIC CURVE OF A VIBRATING CANTILEVER BEAM

By SCOTT H. SIMPKINSON, LAUREL J. EATHERTON, and MORTON B. MILLENSON

SUMMARY

A study was made to determine the effect of rotation on the dynamic-stress distribution in vibrating cantilever beams. The results of a mathematical analysis are presented together with experimental results obtained by means of stroboscopic photographs and strain gages. The theoretical analysis was confined to uniform cantilever beams; the experimental work was extended to include a tapered cantilever beam to simulate an aircraft propeller blade. Calculations were made on a non-dimensional basis for second- and third-mode vibration; the experiments were conducted on beams of various lengths, materials, and cross sections for second-mode vibration. From this investigation it was concluded that high vibratory-stress positions are unaffected by the addition of centrifugal force. Nonrotating vibration surveys of blades therefore are valuable in predicting high vibratory-stress locations under operating conditions.

INTRODUCTION

Resonant vibration causes many of the failures encountered in aircraft propeller blades and in currently used high-speed compressor and turbine blades. The high stresses that cause these failures are brought about by the coincidence of one of the exciting forces present with one of the natural frequencies of the blade. Considerable progress has been made on the study of resonant vibration with the introduction of strain gages for measuring stress in rotating parts. This method of measuring vibratory stress in propeller blades has become the standard procedure for determining safe engine-propeller combinations. The results obtained in this manner, however, have sometimes proved unsatisfactory because misleading data have resulted from the improper location of the strain gages. Many propeller-blade fatigue failures have occurred on endurance test stands although the engine-propeller combination had been pronounced safe on the basis of results obtained with strain-gage vibration surveys. Such failures indicate a need for a better method of locating strain gages on propeller blades. The strain gages can be properly located if the location of the high vibratory-stress positions can be determined.

The addition of centrifugal force causes a considerable change in the natural frequencies of a propeller blade. Reference 1 states and theoretical calculations in reference 2 imply that centrifugal force also changes the mode shapes and high-stress positions of a vibrating blade. British investigators (Morris and Head, and Piper) maintain,

however, that centrifugal force has little or no effect on mode shape. If this opinion is correct, a static (nonrotating) vibration survey of a blade would result in the location of the high-stress positions for the various natural modes of vibration. Furthermore, only one static survey would be necessary for a particular type of blade, because geometrically similar blades have the same mode shapes and would therefore have geometrically similar high-stress positions.

In an effort to improve the checking of engine-propeller combinations and to provide a means of predicting vibration trouble in high-speed turbines and compressors, an investigation was conducted at the NACA Cleveland laboratory during 1945 and 1946 to determine the effect of centrifugal force on the mode shape and the stress distribution of a rotating blade vibrating at resonance.

The vibration of uniform beams in a centrifugal-force field was mathematically investigated employing a numerical method given by Myklestad (reference 3) for the determination of natural frequencies and mode shapes of such beams. The problem was experimentally studied by subjecting beams of various lengths and materials to rotational speeds up to 1015 rpm while vibrating in second mode. In addition to beams of uniform cross section, a beam of varying cross section, made to simulate a propeller blade, was also studied. Mode shapes were obtained from photographs taken using a stroboscopic light source and stress-distribution curves were obtained with strain gages. The results of the strain-gage data taken on the tapered beam (nonrotating) were compared with similar data obtained on a propeller blade to determine the similarity in properties of the tapered beam and of a propeller blade.

MATHEMATICAL PROCEDURE AND RESULTS

A convenient method of determining frequencies and mode shapes of rotating beams, such as propeller blades, helicopter rotors, and turbine blades, is given in reference 3. This method involves substituting a series of point masses and massless springs for the beam. The point masses are so selected that the mass distribution of the substitute system represents an approximation of the mass distribution of the actual beam. Similarly, the springs are selected to represent an approximation of the elastic distribution of the beam. Angular and linear deflections of each substitute spring, under the influence of unit loading and unit moment, are used as influence coefficients in the calculation. The

method of calculation is analogous to the more commonly known Holzer method of analyzing torsional vibrations but is somewhat more complicated, particularly when the effect of centrifugal force is introduced. The calculation is made by assuming a natural frequency and computing the angular and linear deflections, point by point, proceeding from the free end of the beam to the fixed end. The assumed frequency is an actual natural frequency if the calculated deflections meet the end conditions at the fixed end. With skill, the correct frequency can be determined after two or three calculations.

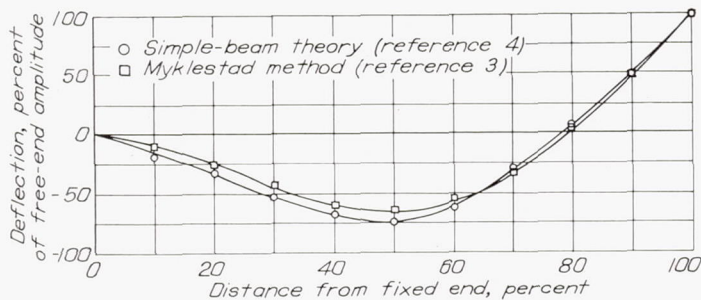


FIGURE 1.—Comparison of calculated second-mode deflection curves for nonrotating uniform cantilever beam.

Although this method represents an approximation of actual conditions, the accuracy of the resulting values is limited only by the number of mass-spring sets used in approximating the beam. All the calculations for this investigation were made using 10 equal concentrated masses located at the midpoints of 10 equal sections of the beam. The accuracy of this approximation is shown in figure 1 where the second-mode deflection curves, calculated by the Mykelstad method (reference 3) and by solution of the theoretical equation based on simple-beam theory given in reference 4, are plotted for a nonrotating uniform canti-

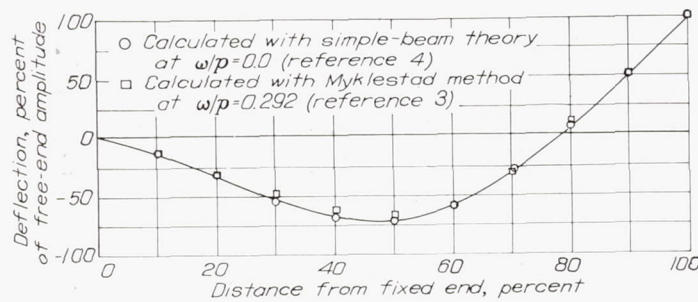


FIGURE 2.—Effect of centrifugal force on second-mode deflection curve of uniform cantilever beam.

lever beam. The Mykelstad method for this degree of approximation accurately determines the critical locations of the deflection curves; namely, the nodes, the antinodes, and the inflection points. Relative amplitudes, however, are somewhat in error.

A plot of the Mykelstad calculation for a uniform cantilever beam vibrating in second mode, while rotating at a speed such that the ratio of angular velocity (radians/sec) to natural angular frequency (radians/sec) ω/p is 0.292, is

shown in figure 2. A deflection curve of a cantilever beam with no rotation, as calculated from the theoretical equation of reference 4, is plotted on the same figure. Figure 3 shows the same type of plot for third-mode vibration. The Myklestad calculation for this figure was made with $\omega/p=0.160$. The two ratios, 0.292 (fig. 2) and 0.160 (fig. 3), represent angular velocities approximately 100 percent above the rotative speeds encountered in operation and were selected to emphasize any effect rotation might have on the location of critical points in the deflection curves.

Figure 2 indicates that no shift of critical points occurs because of rotation. The small shift in antinode positions in figure 3 is attributed to insufficient mass-spring combinations for accuracy at this higher mode of vibration.

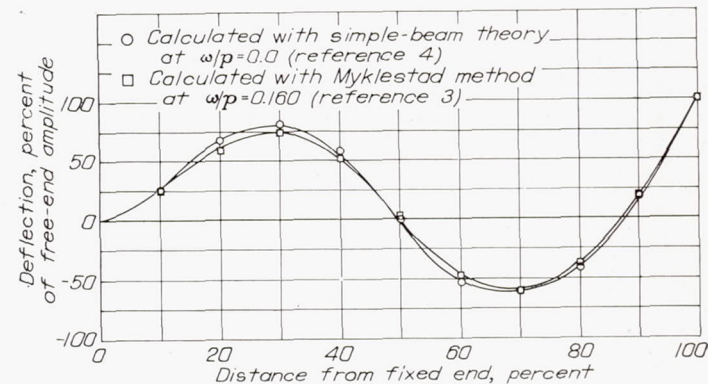


FIGURE 3.—Effect of centrifugal force on third-mode deflection curve of uniform cantilever beam.

APPARATUS AND PROCEDURE

The experimental data were obtained with the apparatus shown in figure 4, which included instruments for recording deflection, angular velocity, and vibration frequency. The

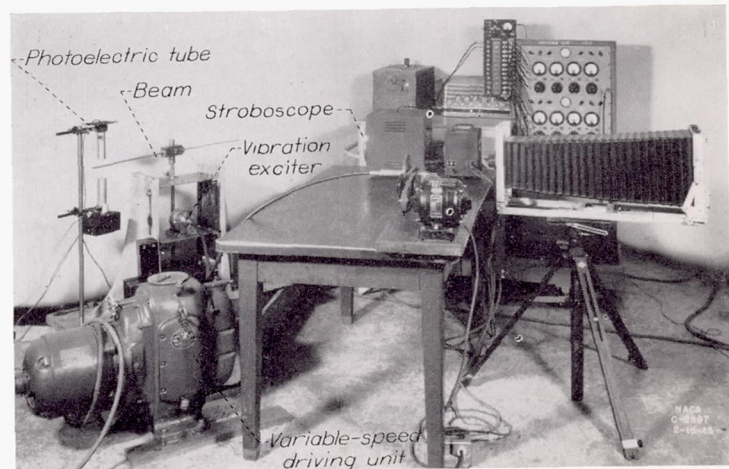


FIGURE 4.—Setup for taking stroboscopic photographs of rotating beam.

setup provided a means of simultaneously vibrating and rotating a beam. A photoelectric tube, which actuated a stroboscope, was used to "stop" the beam for photographing the vibration during rotation. White dots were painted on

the beam to facilitate photographing and measuring. The photoelectric-tube signal was also recorded on an oscillograph for use as a revolution counter. The signal from a vibration pickup located on the bedplate was impressed on another channel of the oscillograph as a simultaneous frequency counter. Strain gages, located as shown in figure 5, were used to obtain vibratory stress-distribution data.

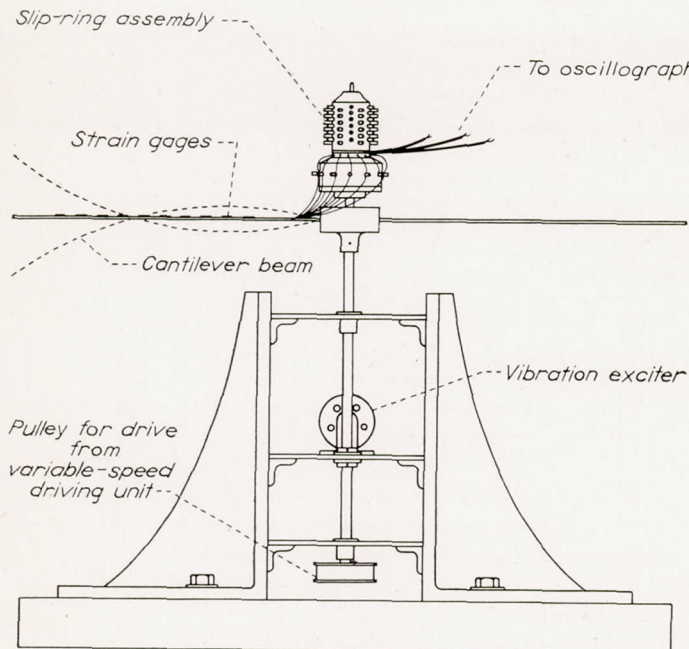


FIGURE 5.—Diagrammatic sketch of setup for measuring vibratory stress along cantilever beam that is simultaneously rotating and vibrating.

Three different beams were used in the experiment. The first beam was of low-carbon steel with a cross section of 1 by $\frac{1}{16}$ inch and had a free length of $17\frac{1}{16}$ inches. The beam was mounted as a cantilever with the fixed end at the center of rotation. Various speeds from 0 to 1015 rpm were set with the variable-speed driving unit. The speed of the exciter was set for resonant second-mode vibration at each of the rotational speeds. A 30-second film exposure was made at each speed and records of the angular velocity and vibration frequency were obtained. The runs were then repeated with the beam enclosed in a transparent plastic box (fig. 6) to eliminate any effect of aerodynamic

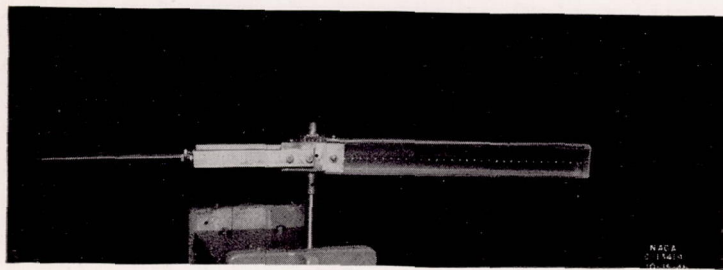


FIGURE 6.—Cantilever beam enclosed in plastic box to eliminate rotational aerodynamic damping effect.

855783—50—2

damping that might accompany combined rotation and vibration.

Strain gages were cemented to the top of the beam. The lead wires were cemented to the top of the beam and run to a slip-ring assembly having 13 channels. The signals from the strain gages were impressed on a multichannel oscillograph capable of simultaneously recording 12 stresses. Records of the vibratory stress were obtained at speeds of 0, 536, and 1015 rpm at second-mode resonance.

The second beam was of soft brass with a cross section of 1 by $\frac{1}{8}$ inch and had a free length of 20 inches. Deflection photographs were taken of this beam at various angular velocities ranging from 0 to 998 rpm.

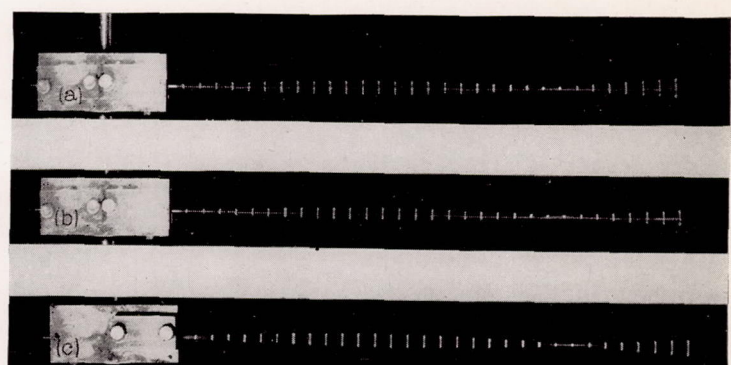
The third beam was of low-carbon steel with a cross section that varied uniformly from 1 by $\frac{3}{16}$ inch at the fixed end to 1 by $\frac{1}{64}$ inch at the free end. The free length of this tapered cantilever beam is $17\frac{1}{4}$ inches. The same type of frequency and mode-shape data was obtained for the tapered beam as for the uniform steel beam.

In order to obtain more complete data on the tapered beam, 18 strain gages were used. Because only 12 gage signals could be recorded at one time, the gages were wired into two groups of 12 gages each, the central 6 gages being common to both sets. One record of each set was taken at each test point. The data from the six common gages were used to correct for small changes in amplitude between readings.

A hollow steel propeller blade was so mounted as to be supported in the same manner as in an actual propeller hub. Strain gages were mounted on the camber side along the maximum camber line. Simultaneous records of bending stress along the blade were obtained with the propeller blade subjected to nonrotating second-mode vibration.

EXPERIMENTAL RESULTS

Photographs of the uniform cantilever steel beam, vibrating in second mode and rotating at speeds of 1015, 536, and 0 rpm, are shown in figure 7. Measurements were made



(a) Rotational speed, 1015 rpm; frequency, 57.9 cycles per second.
 (b) Rotational speed, 536 rpm; frequency, 44.7 cycles per second.
 (c) Rotational speed, 0 rpm; frequency, 38.6 cycles per second.

FIGURE 7.—Stroboscopic photographs of uniform cantilever steel beam fixed at center of rotation and vibrating in second mode at various speeds of rotation.

from enlargements of these photographs and the data are plotted in figure 8. The only change in these curves resulting from an increase in speed of rotation is a decrease in relative antinode amplitude.

The experiment was then repeated with the beam enclosed in the transparent plastic box to eliminate any effects of

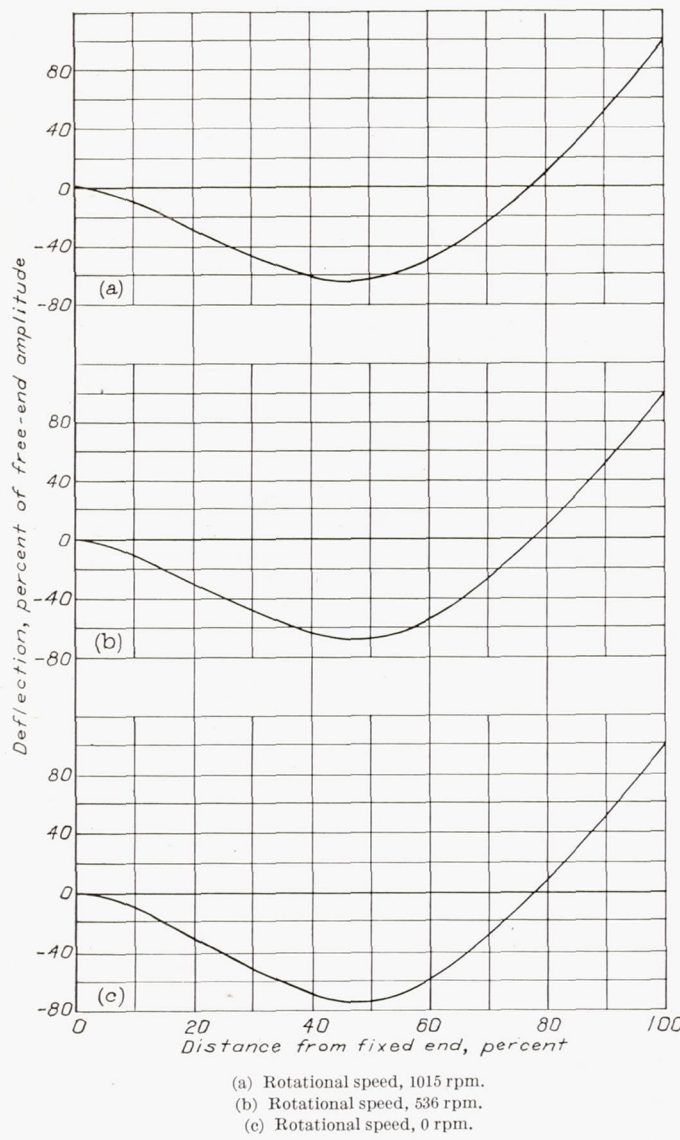


FIGURE 8.—Experimental deflection curves of uniform cantilever steel beam fixed at center of rotation and vibrating in second mode while rotating at various speeds.

rotational aerodynamic damping. When the results of measurements made from enlargements of the photographs shown in figure 9 were plotted, the deflection curves were the same as those obtained with the unenclosed beam. It was therefore concluded that the effect of rotational aerodynamic damping could be neglected in the experiments.

Experimental vibratory stress-distribution curves for the uniform cantilever steel beam were obtained from the second derivatives of the deflection curves shown in figure 8. These stress-distribution curves, together with strain-gage readings, are shown in figure 10.

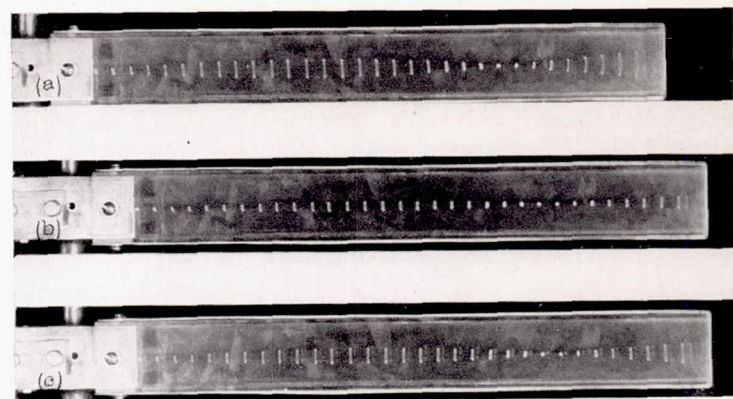


FIGURE 9.—Stroboscopic photographs of uniform cantilever steel beam enclosed in transparent plastic box fixed at center of rotation and vibrating in second mode at various speeds of rotation.

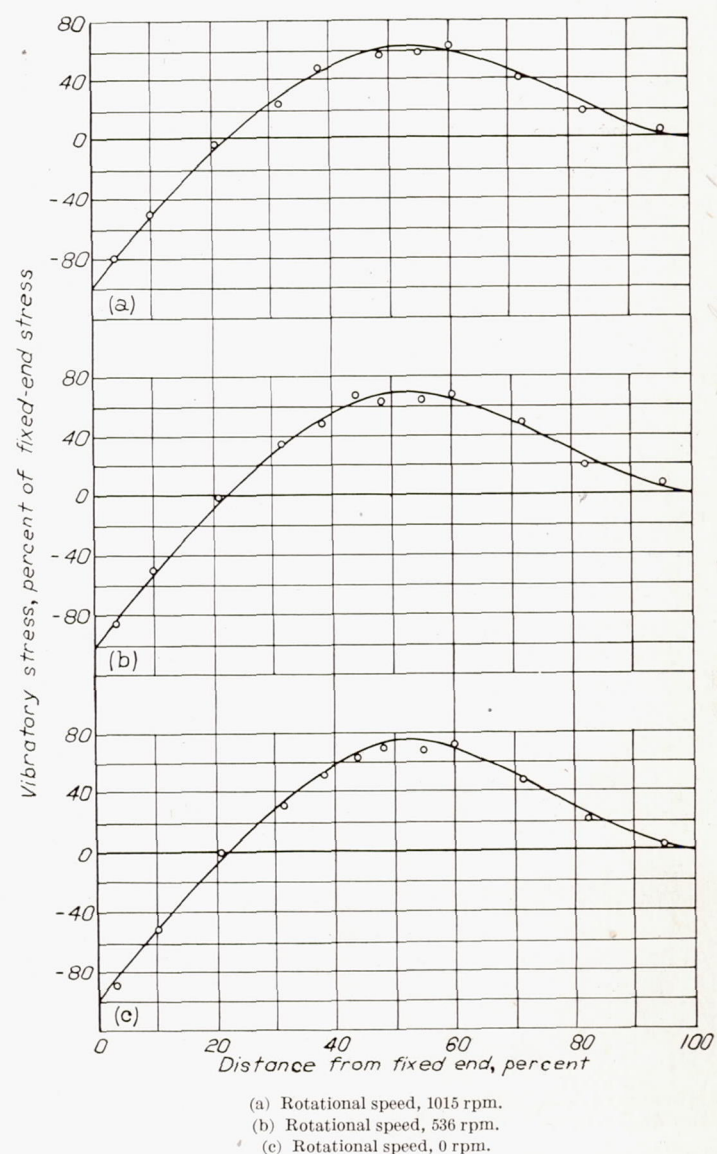


FIGURE 10.—Vibratory stress-distribution curves of uniform cantilever steel beam fixed at center of rotation and vibrating in second mode while rotating at various speeds. Stress curves drawn from second derivative of experimental deflection curves of figure 8. Experimental points obtained from strain-gage readings.

An accurate check of second-mode resonant frequency at various speeds of rotation was made. The frequency was assumed to vary with speed according to the formula (derived from the formula given in reference 5).

$$f = \sqrt{f_0^2 + K\Omega^2}$$

where

- f resonant frequency, cycles per second
- f_0 resonant frequency at 0 rpm, cycles per second
- K constant
- Ω angular velocity of beam, revolutions per second

The value of the constant K for second mode obtained from experimental data was 6.55 as compared with an approximate value of 6 given in reference 5. A comparison of curves obtained by using these two constants is presented in figure 11.

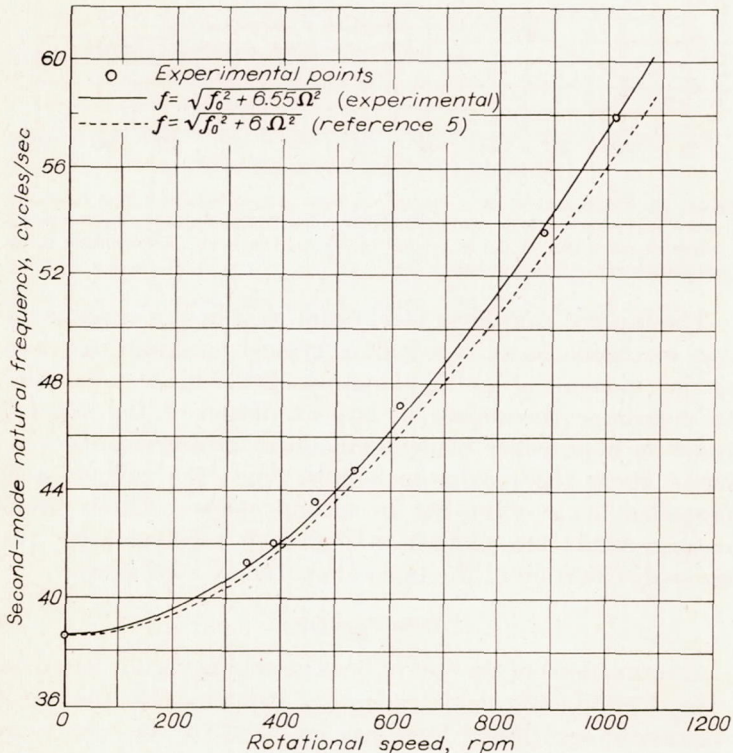


FIGURE 11.—Variation of second-mode natural frequency with rotational speed for uniform cantilever steel beam, $\frac{1}{16}$ inch deep, 1 inch across, and $17\frac{3}{16}$ inches long with fixed end at center of rotation.

In order to eliminate any coincidence involving the material constants or dimensions, a brass beam of different length and cross section was used in the second part of the experiment. Stroboscopic photographs of this beam are presented in figure 12. Deflection measurements made from enlargements of figure 12 are plotted in figure 13 and can be compared with the deflection curves of the uniform cantilever steel beam shown in figure 8. The identical nature of the

two sets of deflection curves for the uniform cantilever brass and steel beams eliminated any necessity for a stress analysis of the brass beam. From these data, it is evident that the



(a) Rotational speed, 998 rpm; frequency, 60.2 cycles per second.

(b) Rotational speed, 525 rpm; frequency, 48.3 cycles per second.

(c) Rotational speed, 0 rpm; frequency, 42.5 cycles per second.

FIGURE 12.—Stroboscopic photographs of uniform cantilever brass beam fixed at center of rotation and vibrating in second mode at various speeds of rotation.

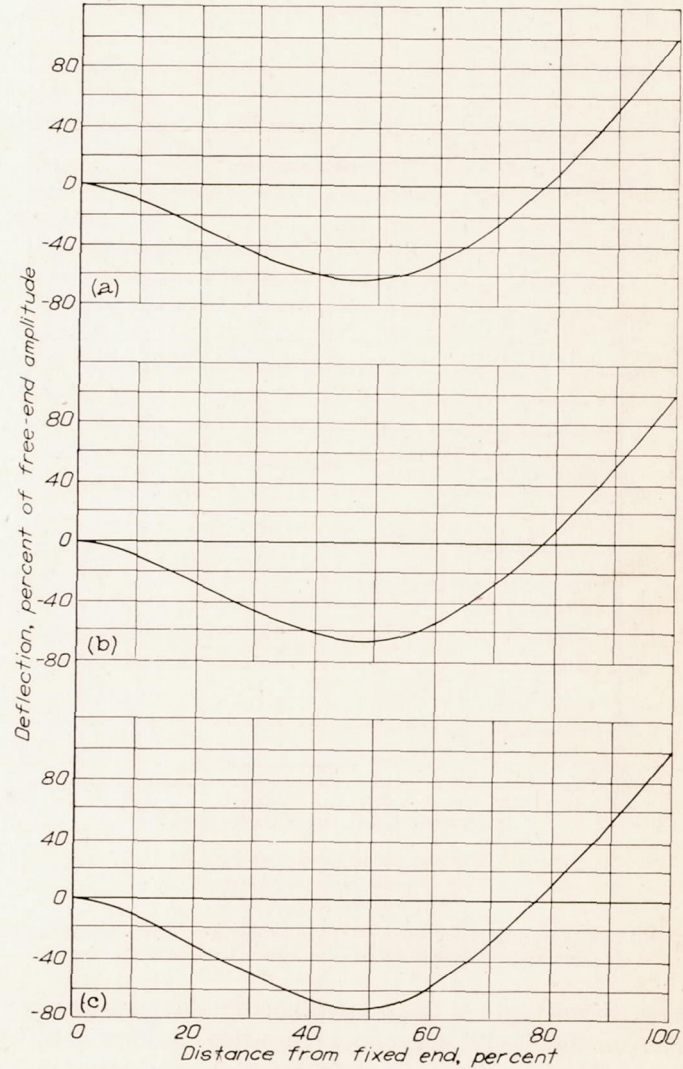
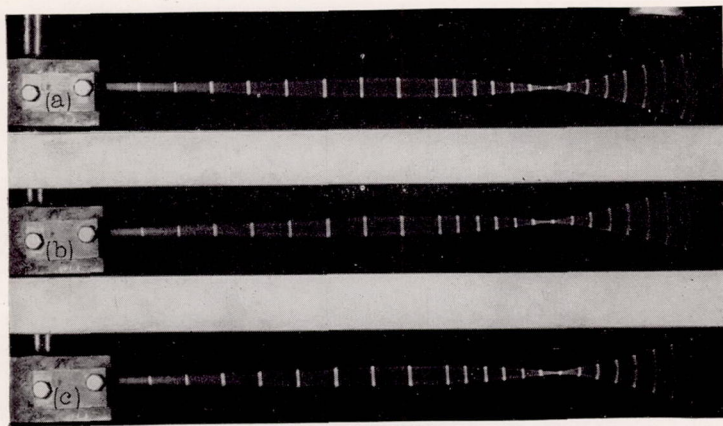


FIGURE 13.—Experimental deflection curves of uniform cantilever brass beam fixed at center of rotation and vibrating in second mode while rotating at various speeds.



(a) Rotational speed, 1010 rpm; frequency, 86.7 cycles per second.
 (b) Rotational speed, 503 rpm; frequency, 81.7 cycles per second.
 (c) Rotational speed, 0 rpm; frequency, 80 cycles per second.

FIGURE 14.—Stroboscopic photographs of tapered cantilever steel beam fixed at center of rotation and vibrating in second mode at various speeds of rotation.

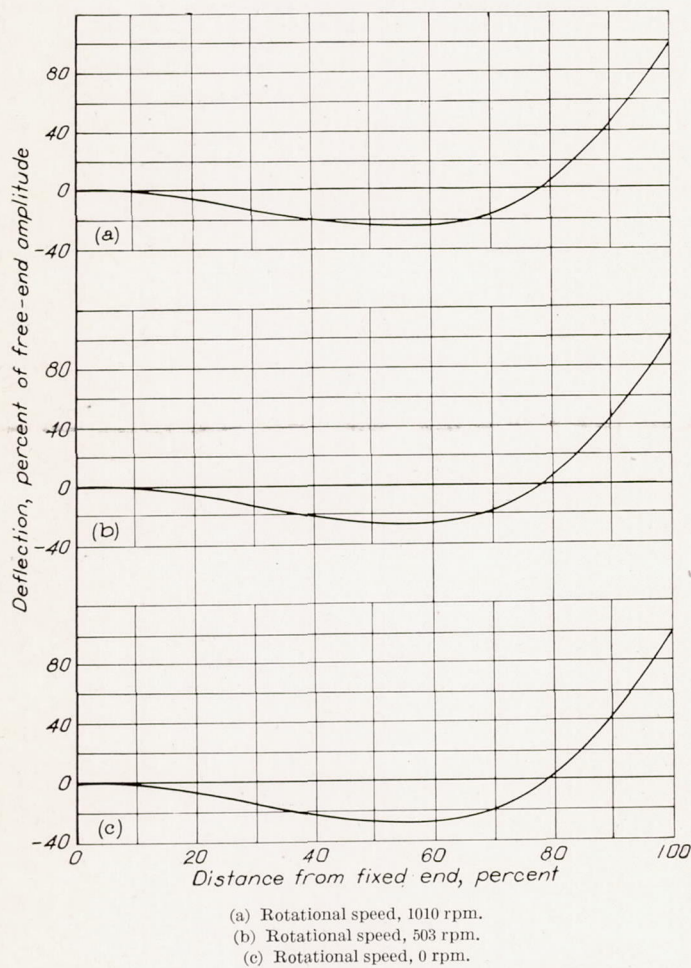


FIGURE 15.—Experimental deflection curves of tapered cantilever steel beam fixed at center of rotation and vibrating in second mode while rotating at various speeds.

physical constants of the material or the dimensions have no effect on the elastic curve of a vibrating uniform cantilever beam. This conclusion is valid for both stationary and rotating beams.

Deflection curves for the tapered cantilever steel beam were

obtained, as in the previous experiments, from the photographs shown in figure 14 and are presented in figure 15. The relation between antinode and tip deflection is considerably changed from the uniform-cantilever-beam relation but the node occurs at the same place, that is, 78 percent of the length from the fixed end. The same tendency in antinode deflection compared with tip deflection occurs with increased angular velocity, as in the case of the uniform cantilever beam; that is, the antinode loop becomes smaller in relation to tip amplitude with increase in angular velocity of the beam. Stress distribution at a rotational speed of 0 rpm was obtained from the second derivative of the deflection curve (fig. 15 (c)) and is plotted in figure 16 with the experimental points obtained from strain-gage readings.

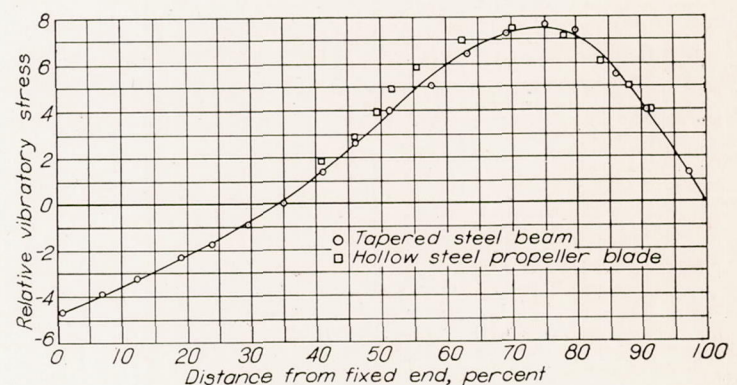


FIGURE 16.—Comparison of stress distribution along tapered cantilever steel beam and hollow steel propeller blade. Stress curve drawn from second derivative of experimental deflection curve (fig. 15 (c)) of tapered cantilever steel beam. Experimental points obtained from strain-gage readings.

The tapered cantilever steel beam used in this experiment was so chosen as to represent a typical variation in cross-section moment of inertia along a propeller blade. In order to determine the degree of approximation of the tapered beam to a propeller blade, strain-gage measurements were made along the maximum camber line of a hollow steel propeller blade vibrating in second mode. These stress measurements are plotted in figure 16 together with the stress distribution of the tapered cantilever steel beam.

DISCUSSION

A comparison of the curves presented in figure 17, based on experimental and calculated results, indicates that the introduction of centrifugal force has no effect on the maximum dynamic-stress locations in a vibrating cantilever beam fixed at the center of rotation within the investigated speed range. The general shape of the deflection curve, in particular the location of node positions, is also unaffected by rotation although relative amplitudes vary; that is, the amplitude of antinode loops relative to tip amplitude decreases with increasing rotational speed. Because node and maximum-dynamic-stress locations are invariant, static-bending-vibration surveys of beams that will be subsequently subjected to vibratory forces in a centrifugal-force field will locate critical areas for strain-gage location in rotary testing. This

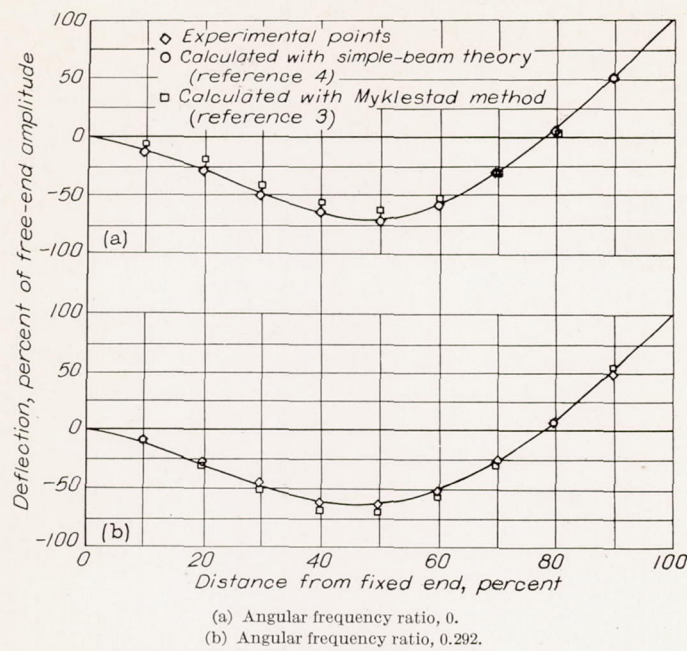


FIGURE 17.—Comparison of theoretical and experimental curves showing second-mode deflections of uniform cantilever beam for two rotations.

procedure will decrease the possibility of misleading data because of improperly located strain gages.

CONCLUSIONS

Two important conclusions may be drawn on the basis of the study of beams vibrating in a centrifugal-force field:

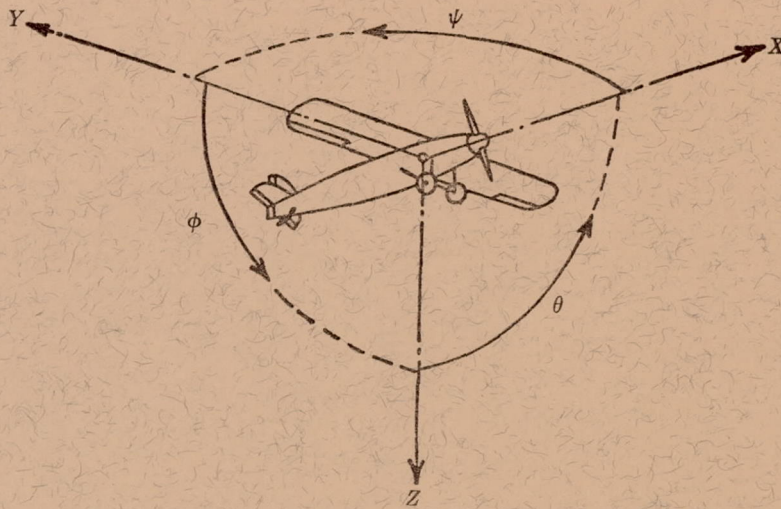
1. Node positions and maximum-vibratory-stress locations are unaffected by centrifugal force within the investigated speed range in a cantilever beam fixed at the center of rotation and vibrating in bending modes.

2. Static-vibration surveys of propeller blades and similar rotating parts may be utilized to predict the maximum vibratory-stress positions in such blades under operating conditions.

AIRCRAFT ENGINE RESEARCH LABORATORY,
NATIONAL ADVISORY COMMITTEE FOR AERONAUTICS,
CLEVELAND, OHIO, September 18, 1946.

REFERENCES

1. Theodorsen, T.: Propeller Vibrations and the Effect of the Centrifugal Force. NACA TN No. 516, 1935.
2. Ramberg, Walter, and Levy, Sam: Calculation of Stresses and Natural Frequencies for a Rotating Propeller Blade Vibrating Flexurally. Res. Paper 1148, Nat. Bur. Standards Jour. Res., vol. 21, no. 5, Nov. 1938, pp. 639-669.
3. Myklestad, N. O.: Vibration Analysis. McGraw-Hill Book Co., Inc., 1944, pp. 210-214.
4. Timoshenko, S.: Vibration Problems in Engineering. D. Van Nostrand Co., Inc., 2d ed., 1937, pp. 331-345.
5. Den Hartog, J. P.: Mechanical Vibrations. McGraw-Hill Book Co., Inc., 2d ed., 1940, p. 310.



Positive directions of axes and angles (forces and moments) are shown by arrows

| Axis | | Force (parallel to axis) symbol | Moment about axis | | | Angle | | Velocities | |
|--------------|--------|--|-------------------|--------|-----------------------|-------------|--------|--|---------|
| Designation | Symbol | | Designation | Symbol | Positive direction | Designation | Symbol | Linear (compo- nent along axis) | Angular |
| Longitudinal | X | X | Rolling | L | Y → Z | Roll | φ | u | |
| Lateral | Y | Y | Pitching | M | Z → X | Pitch | θ | v | |
| Normal | Z | Z | Yawing | N | X → Y | Yaw | ψ | w | q |

Absolute coefficients of moment

$$C_i = \frac{L}{qbS} \quad C_m = \frac{M}{qcS} \quad C_n = \frac{N}{qbS}$$

(rolling) (pitching) (yawing)

Angle of set of control surface (relative position), δ . (Indicate surface by proper neutral script.)

D Diameter
 p Geometric pitch
 p/D Pitch ratio

V' Inflow velocity
 V_s Slipstream velocity

T Thrust, absolute coefficient $C_T = \frac{T}{\rho n^2 D^4}$

Q Torque, absolute coefficient $C_Q = \frac{Q}{\rho n^2 D^5}$

P Power, absolute coefficient $C_P = \frac{P}{\rho n^3 D^5}$

C_s Speed-power coefficient = $\sqrt[5]{\frac{\rho V^5}{P n^2}}$

n Revolutions per second, rps

Φ Effective helix angle = $\tan^{-1} \left(\frac{V}{2\pi r n} \right)$

5. NUMERICAL RELATIONS

1 hp = 76.04 kg-m/s = 550 ft-lb/sec

1 metric horsepower = 0.9863 hp

1 mph = 0.4470 mps

1 mps = 2.2369 mph

1 lb = 0.4536 kg

1 kg = 2.2046 lb

1 mi = 1,609.35 m = 5,280 ft

1 m = 3.2808 ft